# Unique features of action potential initiation in cortical neurons

Björn Naundorf, Fred Wolf, Maxim Volgushev

## *Online supplementary information (Part 3 of 3):*

## *Cooperative channel activation*

In this part of the Supplementary Information we introduce a model of AP initiation by cooperative activation of voltage-gated sodium channels and characterize its basic properties. Then we describe the computational consequences of the characteristic features of cortical action potential initiation. Using a novel phenomenological neuron model, we show that these features allow a neuronal population to encode rapidly varying signals and to suppress responses to slowly varying stimuli.

## Contents

## AP initiation with cooperative sodium channel activation

The large AP onset rapidness typical of cortical APs suggests that during the initial phase of APs, sodium channels open in a coordinated fashion. To investigate whether cooperative sodium channel activation can quantitatively explain the co-occurrence of a large AP onset span and a large AP onset rapidness, we constructed and analysed a model for AP generation, in which sodium channel activation could be varied between independent and cooperative gating. In the model, individual sodium channels open (close) either independently of each other or cooperatively, i.e. the opening (closing) of one channel increases the probability of neighbouring sodium channels to also open (close). Our model is based on a model of single sodium channel gating introduced by Aldrich, Corey and Stevens (1983). The single channel model incorporates state-dependent inactivation from the open state, voltage-dependent inactivation from the closed state and is consistent with sodium channel activation curves and channel open times obtained from patch recordings (Aldrich, Corey and Stevens 1983; Martina and Jonas 1997). In the cooperative activation model, an individual channel $i$ is coupled to $K$ neighbouring channels such that the opening of each of them shifts the activation curve of channel $i$ by a voltage shift $-J$ towards more hyperpolarized values. With $J = 0mV$, the model describes statistically independent single channel activation. With $J > 0mV$, channels are activating in a cooperative fashion. To model AP generation, mean field equations for the resulting sodium current were incorporated into the current balance equation of a membrane compartment. The compartment contained - besides the sodium channels - a large leak conductance. For simplicity, the model contains no voltage dependent potassium channels as their inclusion leaves the nature of AP onsets unaffected but complicates the analysis. In the following, we describe the

construction of the model and its main properties. As shown in the paper and below, (1) there is a critical coupling strength above which the current voltage relationship of an ensemble of sodium channels exhibits a step-like activation, deviating from the activation curve of an isolated channel. (2) In a neuronal membrane this leads to the generation of APs exhibiting a large onset rapidness. (3) Voltage-dependent inactivation from closed states and slow deinactivation of sodium channels lead to a large AP onset span. The model, thus does not exhibit an antagonism between AP onset rapidness and onset variability.

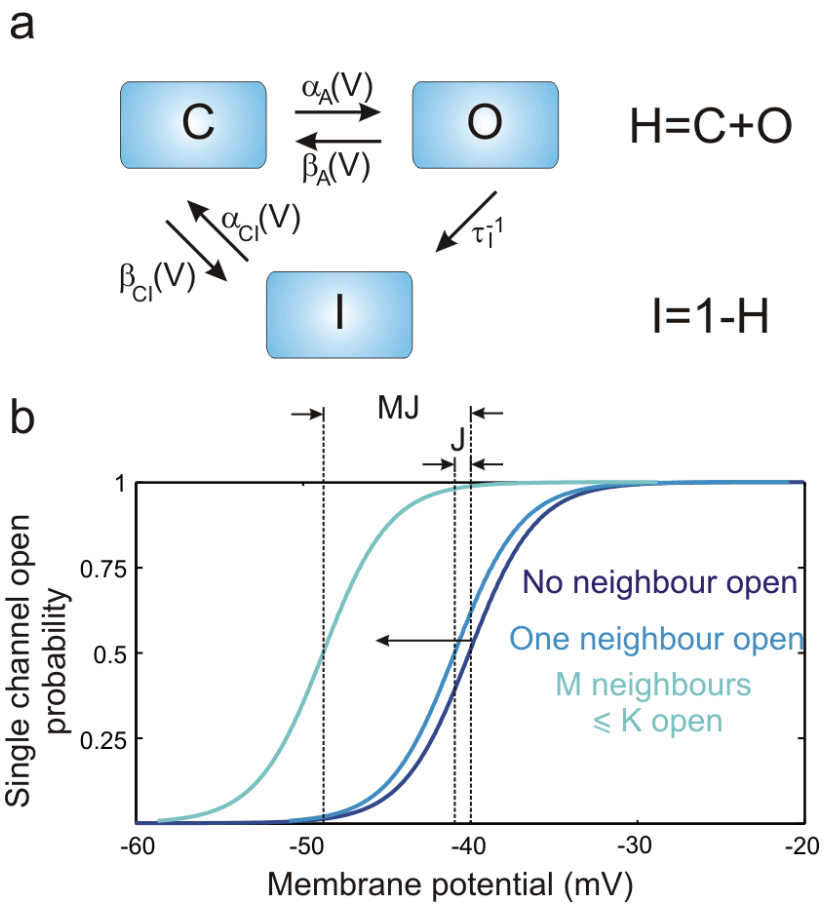


Figure 3SI (a) State transition scheme of the single sodium channel model. (b) Modelling inter-channel cooperativity: In the coupled model, the opening of neighbouring channels shifts the single channel activation curve to more hyperpolarized potentials such that the probability of channel opening at a given MP is increased.

## The single channel model

Our model of cooperative sodium channel activation is based on a single channel model originally introduced by Aldrich, Corey and Stevens (1983). Its state transition scheme (Fig. 3SI a) has three states: *open*, *closed* and *inactivated* and incorporates three types of state transitions: voltage-dependent activation and deactivation, voltage-independent inactivation from the open state, and voltage-dependent

inactivation from the closed state and de-inactivation from the inactivated to the closed state.

Voltage-independent inactivation from the open state occurs with rate $\tau_I^{-1}$.

Transitions between closed and open states and between inactivated and closed states occur with rates $\alpha_A(V)$ (opening), $\beta_A(V)$ (closing) and $\alpha_{CI}(V)$ (de-inactivation), $\beta_{CI}(V)$ (inactivation), respectively (Fig. 3SI a). The dynamics of a population of such channels is described by kinetic equations for the fraction of open channels $O(t)$ and the fraction of available channels $H(t)$

$$\dot{O}(t) = \alpha_A(V)\big(H(t) - O(t)\big) - \big(\tau_I^{-1} + \beta_A(V)\big)O(t)$$
$$\dot{H}(t) = \alpha_{CI}(V)\big(1 - H(t)\big) - \beta_{CI}(V)\big(H(t) - O(t)\big) - \tau_I^{-1}O(t)$$

For discussing model properties it is useful to consider two characteristic functions: The instantaneous single channel activation curve, $o_\infty(V)$ and the equilibrium inactivation function $I_\infty(V)$. If the time scale of activation is shorter than the inactivation time constant $\tau_I$, the activation of channels from the available fraction, $H(t)$, is described by the instantaneous single channel activation curve

(13) $$o_\infty(V) = \alpha_A(V) / \big(\alpha_A(V) + \beta_A(V)\big).$$

For constant membrane potential and negligible sodium channel activation, the equilibrium inactivation function

(14) $$I_\infty(V) = \beta_{CI}(V) / \big(\alpha_{CI}(V) + \beta_{CI}(V)\big)$$

describes the equilibrium fraction of inactivated channels as a function of membrane potential.

## Mean field model of cooperative gating

Based on the above model of single channel gating we formulated a mean field model of cooperative sodium channel activation. To derive this model, we assumed that each channel is coupled to $K$ neighbouring channels. Opening of any of these neighbours is then assumed to cause a shift of the instantaneous activation curve of the channel by $-J$ towards lower membrane potentials. The activation and deactivation rates of channel $i$ are then,

$$\begin{aligned} \alpha_i^A(V) &= \alpha_A(V + \sum_j J_{ij}\sigma_j) \\ \beta_i^A(V) &= \beta_A(V + \sum_j J_{ij}\sigma_j) \end{aligned} \tag{15}$$

where $J_{ij} = J$ if channels $i$ and $j$ are coupled, $J_{ij} = 0$ else, and $\sigma_j$ is a binary single channel state variable labelling channels in the open state: $\sigma_j = 1(0)$ if channel $j$ is open (not open). A mean field model of cooperative channel gating is obtained by replacing the voltage shift term $\sum_j J_{ij}\sigma_j$ by its population average $KJO(t)$. The dynamics of the open and available fractions are then,

$$\begin{aligned} \dot{O}(t) &= \alpha_A(V + KJO(t))\big(H(t) - O(t)\big) - \big(\tau_I^{-1} + \beta_A(V + KJO(t))\big)O(t) \\ \dot{H}(t) &= \alpha_{CI}(V)\big(1 - H(t)\big) - \beta_{CI}(V)\big(H(t) - O(t)\big) - \tau_I^{-1}O(t) \end{aligned} \tag{16}$$

.

The case of independent gating is recovered if the coupling strength is set to zero, $J = 0$. For $J > 0$, the cooperative case, the dynamics of the open and available fraction does not passively follow the voltage time-course but contains a positive feedback interaction between sodium channels.

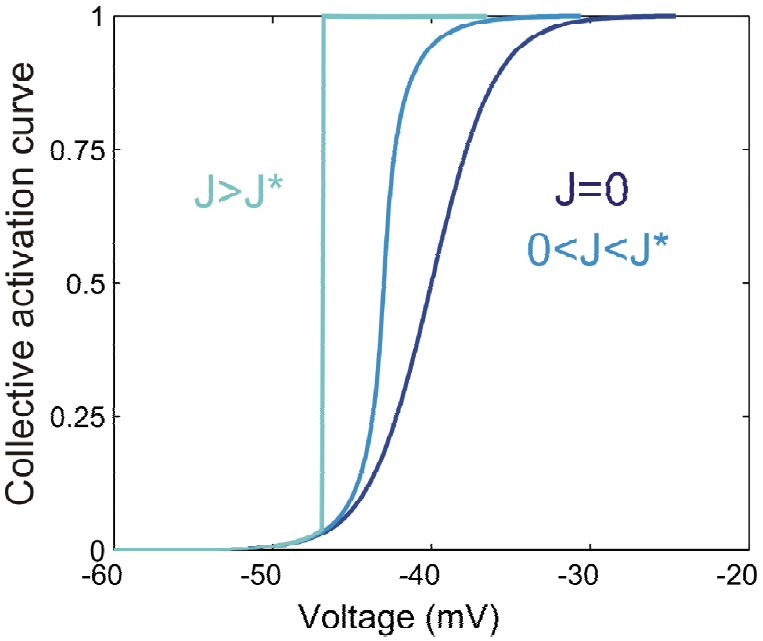


Figure 4SI: Schematic representation of the collective activation curves of sodium channels for varying degrees of inter-channel coupling.

## The collective sodium activation curve

The impact of cooperative gating is revealed by considering the fraction of open sodium channels relative to the available fraction, as a function of the MP for $\tau_I^{-1} = 0$, subsequently called the *collective sodium activation curve*. Assuming a temporally constant available fraction $H_0$, the collective sodium activation curve satisfies the equation

(17) $$o_\infty^J(V) = o_\infty(V + H_0 K J o_\infty^J(V)),$$

where $o_\infty(V)$ is the instantaneous activation curve of independent channels. This equation is a self-consistency relation for $o_\infty^J(V)$. In the uncoupled case, $J = 0$, the collective sodium activation curve equals the single channel activation curve. For $J > 0$, the collective sodium activation curve $o_\infty^J(V)$ becomes progressively steeper than $o_\infty(V)$ with increasing values of $J$ and develops a discontinuous jump at a critical potential $V^*$ when the coupling strength $J$ becomes larger than a critical

value $J^*$ (Fig. 4SI). This means that for a supercritical coupling $J > J^*$, a small increase in MP can cause the opening of a macroscopically large fraction of sodium channels, indicating a phase transition in the collective behaviour of the population of channels.

## AP generation with cooperative sodium channels

To study the impact of cooperative sodium channel activation on the generation of APs we incorporated the current mediated by the population of coupled sodium channels, $I_{Na}(t) = g_{Na} O(t)\left(V_{NA} - V(t)\right)$, where $g_{Na}$ is the sodium peak conductance, and $V_{Na}$ the sodium current reversal potential, and a leak current $I_L(t) = g_L\left(V_L - V(t)\right)$, with the leak conductance $g_L$ and the reversal potential $V_L$, into the current balance equation for a membrane compartment of capacitance $C_M$. We simulated this system driven by a fluctuating input current which was modelled by an Ornstein-Uhlenbeck process. The dynamics of the compartment is described by the following system of differential equations:

$$
\begin{aligned}
&\tau\, \dot{z}(t) = -z(t) + \sqrt{\tau}\eta(t) \\
&c_M \dot{V}(t) = g_L\left(V_L - V(t)\right) + g_{Na} O(t)\left(V_{NA} - V(t)\right) + I_0 + \sigma z(t) \\
&\dot{O}(t) = \alpha_A(V + KJO(t))\left(H(t) - O(t)\right) - \left(\tau_I^{-1} + \beta_A(V + KJO(t))\right)O(t) \\
&\dot{H}(t) = \alpha_{CI}(V)\left(1 - H(t)\right) - \beta_{CI}(V)\left(H(t) - O(t)\right) - \tau_I^{-1} O(t)
\end{aligned}
\qquad (20)
$$

where $\tau$ is the correlation time of the input current, $I_0$ its average value, and $\sigma$ its standard deviation.

## Rate functions and parameters

The rate functions describing individual sodium channel activation / deactivation and inactivation / deinactivation where chosen as,

$$
\begin{aligned}
\alpha_A(V) &= \tau_A^{-1}\left(1+\exp\left(-\left(V-V_{1/2}^A\right)/k^A\right)\right)^{-1} \\
\beta_A(V) &= \tau_A^{-1}\left(1+\exp\left(\left(V-V_{1/2}^A\right)/k^A\right)\right)^{-1} \\
\alpha_{CI}(V) &= \tau_{CI}^{-1}\left(1+\exp\left(-\left(V-V_{1/2}^{CI}\right)/k^{CI}\right)\right) \\
\beta_{CI}(V) &= \tau_{CI}^{-1}\left(1+\exp\left(\left(V-V_{1/2}^{CI}\right)/k^{CI}\right)\right)
\end{aligned}
\tag{21}
$$

With this choice the instantaneous single channel activation curve, and the equilibrium inactivation function are of sigmoidal shape

$$
\begin{aligned}
o_\infty^A(V) &= \left(1+\exp\left(\left(V-V_{1/2}^A\right)/k^A\right)\right)^{-1} \\
I_\infty(V) &= \left(1+\exp\left(\left(V-V_{1/2}^{CI}\right)/k^{CI}\right)\right)^{-1}
\end{aligned}
\tag{22}
$$

and the relaxation times for the two transitions (considered independently) are voltage-independent constants $\tau_A$ and $\tau_{CI}$.

Figure 5 of the paper shows numerical simulations of the model for parameter values

$V_{1/2}^A = -35mV, k^A = 6mV, \tau_A = 0.1ms, \tau_I = 0.5ms, V_{1/2}^{CI} = 80mV, k^{CI} = 4mV, \tau_{CI} = 30mV$

of the uncoupled activation dynamics and

$\tau = 50ms, C_M = 1\mu F/cm^2, g_L = 2mS/cm^2, V_L = -80mV, g_{Na} = 68.4mS/cm^2, V_{Na} = 50mV,$
$I_0 = 0\mu A/cm^2, \sigma = 12\mu A/cm^2$
of the currents and conductances.

With these parameters, the single channel activation curve is consistent with results obtained from patch recordings. Inactivation from the closed state has a broad voltage dependence and a relatively large timescale, leading to substantial fluctuation of the level of inactivation even in the absence of AP activity. For Fig. 5a, the coupling strength was chosen supercritical $J = 3.2mV, K = 1000$ leading to a discontinuous current voltage relationship. In Figure 5 of the paper, numerical simulations of the model obtained for these parameters are compared to simulations without cooperativity $J = 0$ (Fig.5b), and with a fast and voltage-independent

deinactivation and inactivation from the closed state $J = 0, \tau_{CI} = 4ms, V_{1/2}^{CI} = 80mV$ (Fig.5c).

The impact of the coupling on the onset potential variability is depicted in Fig. 5SI. The AP onset potential variability is determined by the available fraction of channels.

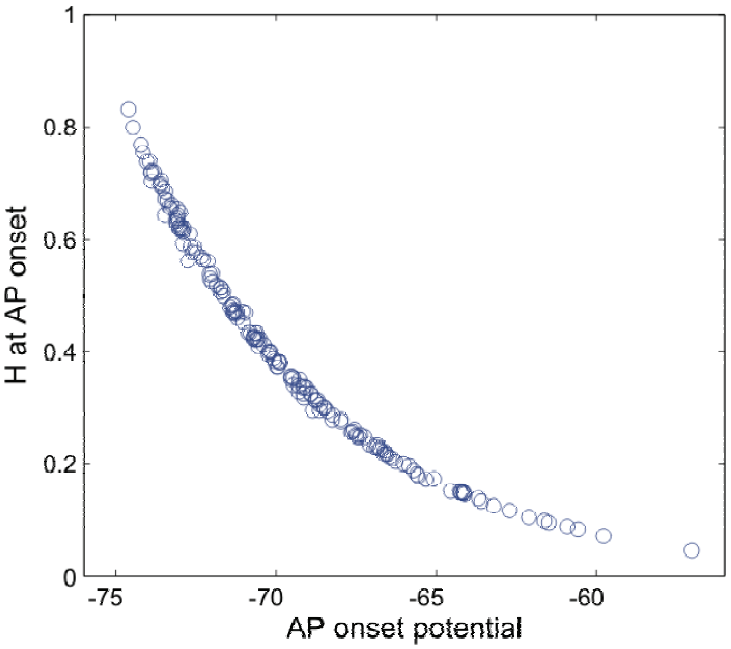


Fig 5SI: Impact of the channel coupling on onset potential variability. The AP onset potential is determined by the available fraction of channels *H*.

## Functional consequences of 'anomalous' AP initiation

To understand the functional implications of a sharp AP onset in combination with a variable onset potential we formulated a phenomenological neuron model capturing the salient features of cortical AP initiation and analyzed its dynamical response properties when driven by fluctuating inputs. We idealized the rapid onset of APs at variable onset potentials by assuming that an AP is initiated instantaneously when the MP reaches a time-dependent threshold potential. The dynamics of the threshold potential was constructed to reproduce a key feature of the statistics of AP onset potentials: A large fraction of the AP onset variability is explained by a correlation between the onset potential and the mean MP preceding an AP (Henze & Buzsaki,

2001, Azouz &Gray 2003). The model shows that the large and history dependent fluctuations in AP onset potential equip a neuron with high pass filter characteristics and therefore with a very effective way of suppressing responses to slowly varying inputs.

The phenomenological model has two degrees of freedom: The MP $V(t)$ and a time-dependent firing threshold $\theta(t)$. The MP consists of two components: A Gaussian stochastic process $u(t)$ with the properties:

$$(23)\ \langle u(t)\rangle = V_0,\ \langle u(t)^2\rangle = {\sigma_V}^2,$$
$$(24)\ \langle \dot{u}(t)\rangle = 0,\ \langle \dot{u}(t)^2\rangle = {\sigma_{\dot{V}}}^2,$$

where the dots denote the first temporal derivative. The second part is a low-pass filtered time dependent signal $f(t)$, where the filter frequency is given by the inverse relaxation time constant of the membrane $\tau_M$:

$$(25)\qquad \tau_M \dot{f}(t) = -f(t) + Signal(t)$$

Each time the MP crosses the threshold $\theta(t)$ from below, i.e. with a rate of change $\dot{V}(t) > 0$, a spike is emitted. Because in the regime considered here, the correlation time is much shorter than the mean time between two adjacent APs, we didn't incorporate an explicit afterhyperpolarization into the model.
The dynamics of the threshold is modelled by a first order kinetics, driven by the MP $V(t)$ with a time constant $\tau_\theta$:

(26) $\tau_\theta \dot{\theta} = (\theta_0 - \theta) + c(V(t) - V_0)$

where $\theta_0$ is the threshold voltage and $c$ the coupling between the threshold and the MP. Since we model the MP as a stochastic process, we will consider in the following an ensemble of such neurons and ensemble averaged quantities. For each neuron in this ensemble the MP fluctuations are independent, every neuron, however, receives the same input $f(t)$. The coding of this input by the ensemble averaged firing rate is the quantity studied.

The average number of APs in the ensemble of neurons in a time interval $(t, t + \Delta t)$ is given by:

(27) $\langle N \rangle = \left\langle \int_t^{t+\Delta t} dt' \delta(u(t') - \theta(t')) \left|\dot{u}(t')\right| \Theta(\dot{u}(t')) \right\rangle$

(28) $= \int_t^{t+\Delta t} dt' \left\langle \delta(u(t') - \theta(t')) \left|\dot{u}(t')\right| \Theta(\dot{u}(t')) \right\rangle$

(29) $= \int_t^{t+\Delta t} dt' \nu(t'),$

where the angular brackets $\langle \bullet \rangle$ denote the average over the ensemble. In the last equation we have introduced the time dependent firing rate $\nu(t)$, which is thus given by:

(30) $\nu(t) = \int_{-\infty}^{\infty} du(t)\, d\dot{u}(t)\, \delta(u(t) - \theta(t)) \left|\dot{u}(t)\right| \Theta(\dot{u}(t))\, P(u(t), \dot{u}(t) \mid t)$

Here $\delta(\bullet)$ denotes the Dirac distribution, $\Theta(\bullet)$ is the Heaviside function and the dots denote the first temporal derivatives. The time dependent joint probability density of

$u(t)$ and $\dot{u}(t)$ at time $t$, $P(u(t),\dot{u}(t)\,|\,t)$, is given by:

$$(31)\quad P(u(t),\dot{u}(t)\,|\,t) = (2\pi\sigma_V\sigma_{\dot{V}})^{-1}\exp\left\{-\frac{1}{2}\left(\frac{u(t)+f(t)}{{\sigma_V}^2}+\frac{\dot{u}(t)+\dot{f}(t)}{{\sigma_{\dot{V}}}^2}\right)\right\}$$

To study the response of the model to dynamically changing inputs, we assumed that the time dependent input signal is given by a cosine with amplitude $A$ and frequency $\omega$. The function $f(t)$ is then given as:

$$(32)\quad f(t) = \frac{A{\tau_M}^{-2}}{{\tau_M}^{-2}+\omega^2}\left(\cos(\omega t)+\tau_M\omega\sin(\omega t)\right)$$

Since the threshold time constant $\tau_\theta$ is typically much larger than the membrane time constant, the threshold dynamics is approximated by:

$$(33)\quad \theta(t) = Ak\tau_M\frac{(1-\tau_M\tau_\theta\omega^2)\cos(\omega t)+(\tau_M+\tau_\theta)\omega\sin(\omega t)}{(1+{\tau_M}^2\omega^2)(1+{\tau_\theta}^2\omega^2)}+\theta_0$$

Evaluating the integral in Eq. (30) with this approximation we obtain an expression for the time dependent firing rate:

(34)

$$\nu(t) = (2\pi\sigma_V)^{-1}\exp\left(-\frac{(f(t)-\theta(t))^2}{2{\sigma_V}^2}\right)\left\{\sigma_{\dot{V}}\exp\left(-\frac{\dot{f}(t)^2}{2{\sigma_{\dot{V}}}^2}\right)+\sqrt{\frac{\pi}{2}}\dot{f}(t)(1+\mathrm{erf}(\dot{f}(t)/(\sqrt{2}\sigma_{\dot{V}}))\right\}$$

To study the response for small values of $A$ we expand $\nu(t)$ in powers of $A$, giving the rate modulation in linear response approximation:

$$(35)\quad \nu(t) = \nu_0 + A\nu_1(\omega)\cos(\omega t + \varphi) + O(A^2),$$

with:

$$(36)\qquad \nu_0 = \frac{\sigma_V}{2\pi\sigma_{\dot V}}\exp\left(-\frac{\theta_0^{\,2}}{2\sigma_V^{\,2}}\right)$$

$$(37)\quad \nu_1(\omega) = \exp\left(-\frac{\theta_0^{\,2}}{2\sigma_V^{\,2}}\right)\frac{\left(\pi\omega^2(1+\tau_\theta^{\,2}\omega^2)\sigma_V^{\,4} + 2\theta_0\sigma_{\dot V}(\sqrt{2\pi}c\tau_\theta\omega^2\sigma_V^{\,2} + \theta_0((k-1)^2 + \tau_\theta^{\,2}\omega^2)\sigma_{\dot V})\right)^{1/2}}{\sqrt{8}\pi\sigma_V^{\,3}\left((1+\tau_M^{\,2}\omega^2)(1+\tau_\theta^{\,2}\omega^2)\right)^{1/2}}$$

$$(38)\quad \varphi(\omega) = \arctan\left(-\frac{\omega(\sqrt{2\pi}(1+\tau_\theta^{\,2}\omega^2)\sigma_V^{\,2} + 2\theta_0(k\tau_\theta + \tau_M(c-1-\tau_\theta\omega^2))\sigma_{\dot V})}{\sqrt{2\pi}\tau_M\omega^2(1+\tau_\theta^{\,2}\omega^2)\sigma_V^{\,2} + 2\theta_0(1-c+\tau_\theta(k\tau_M+\tau_\theta)\omega^2)\sigma_{\dot V}}\right)$$

In the limit $\omega \to \infty$, the amplitude of the rate modulation $\nu_1(\omega)$ becomes constant and independent of $c$:

$$(39)\quad \nu_1(\omega\to\infty) = (\sqrt{8}\pi\tau_M\sigma_V)^{-1}\exp\left(-\frac{\theta_0^{\,2}}{2\sigma_V^{\,2}}\right),$$

the phase lag $\varphi(\omega \to \infty)$ goes to zero.

This means, that even for very high stimulation frequencies, the model will respond to the input with a finite amplitude of the firing rate response, although the amplitude of $f(t)$ and $\theta(t)$ approaches zero for $\omega \to \infty$. This apparently counterintuitive result can be understood from the equation for the instantaneous firing rate (Eq. 34). It does not only incorporate the functions $f(t)$ and $\theta(t)$, but also the temporal

derivative $\dot{f}(t)$ which has a finite high-frequency limit. The finite high-frequency limit of the response function reflects the idealization of a sharp AP threshold, i.e. AP initiation with infinite AP onset rapidness. Models with finite AP onset rapidness in general exhibit a cut-off frequency, which depends on AP onset rapidness and increases when AP onset rapidness is increased (Fig. 6SI; Fourcaud 2003, Naundorf et al., 2005).

In the limit $\omega \to 0$, $\nu_1(\omega)$ is given by:

(40) $\nu_1(0) = \sqrt{2/\pi}(c-1)\frac{\theta_0 \tau_M \sigma_{\dot{V}}}{{\sigma_V}^2}\nu_1(\infty)$,

and the phase lag $\varphi(0)$ is zero.

These results show that the suppression of slowly varying inputs by the threshold variability in combination with the facilitation of the response at high frequencies by a high onset rapidness, equips a neuron model with high-pass filter characteristics. It is important to note that at low-frequencies, the amplitude of the rate modulation decreases with an increasing coupling constant $c$ and becomes zero for $c = 1$, i.e. when the threshold is completely coupled to the mean modulation of the MP (Figure 7SI). In this regime, responses to slowly varying inputs are suppressed without a firing response. This behaviour qualitatively differs from the type of high-pass filter characteristic induced by AP-driven spike frequency adaptation (Benda and Herz 2003). With spike frequency adaptation, slowly varying inputs are never completely suppressed (see Eq.5.2 in Benda and Herz 2003).

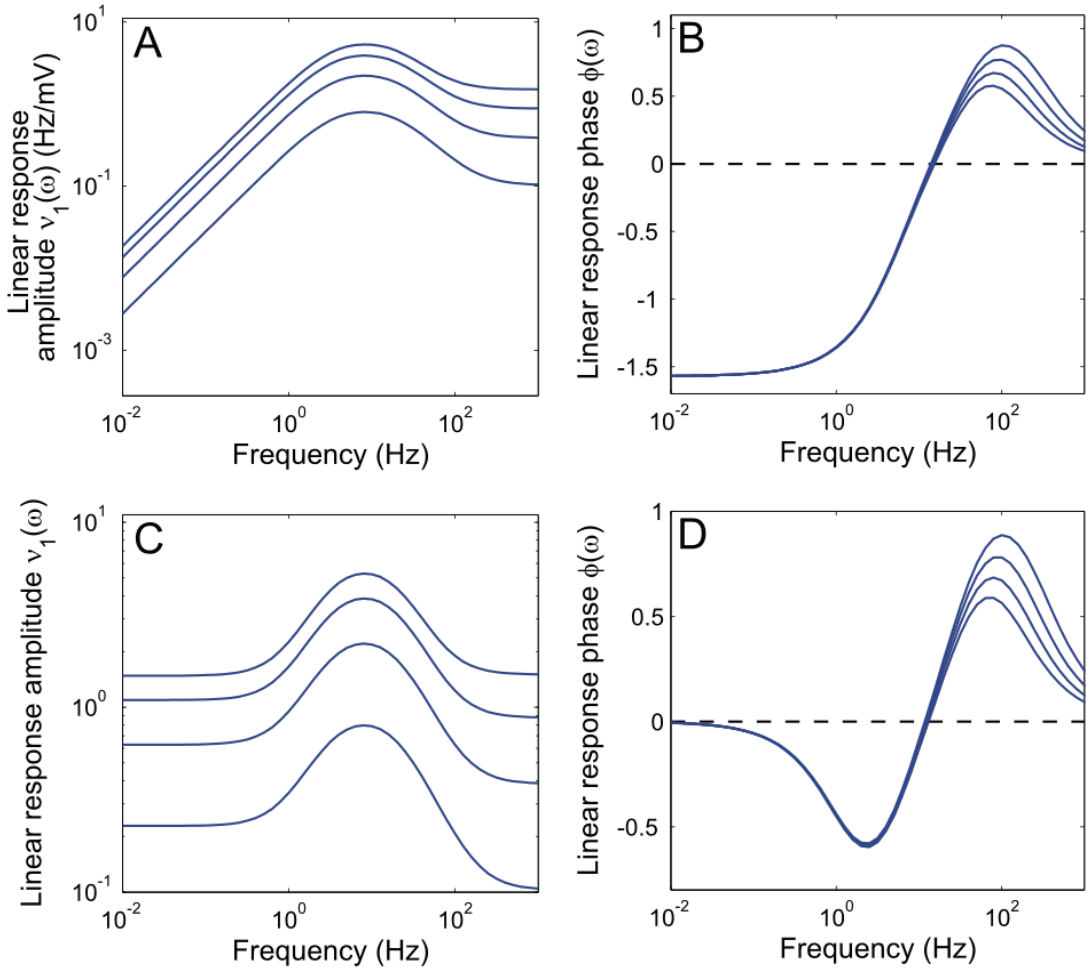


Fig 6SI: Linear response transfer function and phase shift of the $V-\psi$ model. (A) Transmission amplitude $\nu_1(\omega)$ and (B) phase for the case of a fully coupled threshold ($c = 1$) and different stationary firing rates (1 Hz, 5 Hz, 15 Hz, 30 Hz). (C,D) Transmission amplitude and phase for a partially coupled threshold (c=0.75). The transfer functions exhibit a pronounced resonance and settle on a finite value for $\omega \to \infty$. For the case of a fully coupled threshold, the transfer function goes to zero for $\omega \to 0$. Parameters:

$\sigma_V = 1.5, 1.75, 2.0, 2.25\text{mV}$, $\sigma_{\text{dV/dt}} = 1\text{mV/ms}$, $\tau_\psi = 30\text{ms}$, $\psi_0 = 5\text{mV}$.

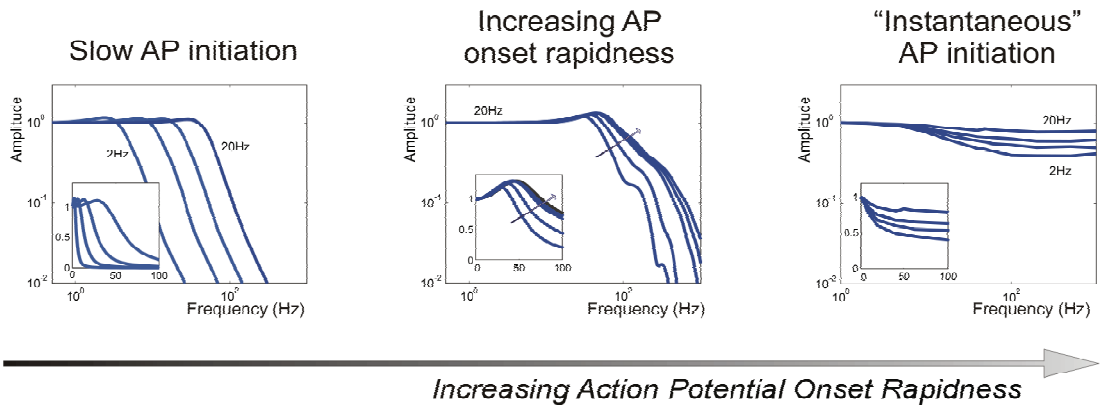


Fig 7SI: Effect of increasing the AP onset rapidness. With increasing onset rapidness, the transmission function shifts to larger values irrespective of the stationary firing rate. For the case of an instantaneous AP onset dynamics (fixed threshold), the transfer function remains finite in the limit $\omega \to \infty$. Curves are labelled for different stationary firing rates. (For details see Naundorf et al., 2005)

## References


Aldrich R..W, Corey D.P., Stevens C.F. A reinterpretation of mammalian sodium channel gating based on single channel recording. *Nature* 306, 436-441 (1983)

Azouz, R., Gray, C.M. Adaptive coincidence detection and dynamic gain control in visual cortical neurons *in vivo*. *Neuron* 37, 513-532 (2003).

Benda J, Herz AV. A universal model for spike-frequency adaptation. Neural Comput. 15, 2523-64 (2003).

Fourcaud-Trocmé, N., Hansel, D., van Vreeswijk, C. & Brunel, N. How spike generation mechanisms determine the neuronal response to fluctuating inputs. *J. Neurosci.* 23, 11628-11640 (2003).

Henze, D.A. & Buzsaki, G. Action potential threshold of hippocampal pyramidal cells in vivo is increased by recent spiking activity. Neurosci. 105, 121-130 (2001).

Martina M, Jonas P. Functional differences in Na+ channel gating between fast-spiking interneurones and principal neurones of rat hippocampus. J Physiol. 505, 593-603 (1997)

Naundorf, B., Geisel T., Wolf F. Action Potential Onset Dynamics and the Response Speed of Neuronal Populations. *J. Comp. Neurosci.* 18, 297-309 (2005).